World Electric Vehicle Journal

MDPI

Article

Efficient Multi-Phase Converter for E-Mobility

Suresh Sampath [1], Zahira Rahiman [1,*], Sharmeela Chenniappan [2], Elango Sundaram [3], Umashankar Subramaniam [4,*] and Sanjeevikumar Padmanaban [5]

1 Department of Electrical Engineering, B S Abdur Rahman Crescent Institute of Science and Technology, Chennai 600 048, India; ssureshavy@gmail.com
2 Department of Electrical Engineering, Anna University, Chennai 600 025, India; sharmeela@annauniv.edu
3 Department of Electrical Engineering, Coimbatore Institute of Technology, Coimbatore 641 014, India; selangocit@gmail.com
4 Renewable Energy Laboratory, Department of Communications and Networks, College of Engineering, Prince Sultan University, Riyadh 11586, Saudi Arabia
5 CTiF Global Capsule, Department of Business Development and Technology, Aarhus University, 7400 Herning, Denmark; sanjeevi_12@yahoo.co.in
* Correspondence: zahirajaved@gmail.com (Z.R.); usubramaniam@psu.edu.sa (U.S.)

Abstract: The recent growth of battery-powered applications has increased the need for high-efficiency step-up dc-dc converters. The step-up conversion is commonly used in several applications, such as electric vehicle (EV); plug-in hybrid electric vehicles (PHEV); photovoltaic (PV) systems; uninterruptible power supplies (UPS); and fuel cell systems. The input current is shared among inductors by paralleling the converters; resulting in high reliability and efficiency. In this paper; a detailed analysis for reducing power loss and improving efficiency is discussed. In continuous conduction mode; the converters are tested with a constant duty cycle of 50%. The multi phase interleaved boost converter (MPIBC) is controlled by interleaved switching techniques; which have the same switching frequency but phases are shifted. The efficiency of the six phase IBC model is 93.82% and 95.74% for an input voltage of 20 V and 200 V, respectively. The presented six phase MPIBC is validated by comparing it with the existing six phase IBC. The result shows that the presented converter is better than the existing converter. The prototype of the two phase and six phase IBC is fabricated to test the performance. It is found that the output power at the load end is highest for the 5 kHz switching frequency.

Keywords: boost converter; interleaved boost converter; multi-phase interleaved boost converter; electric vehicle

Citation: Sampath, S.; Rahiman, Z.; Chenniappan, S.; Sundaram, E.; Subramaniam, U.; Padmanaban, S. Efficient Multi-Phase Converter for E-Mobility. *World Electr. Veh. J.* **2022**, *13*, 67. https://doi.org/10.3390/wevj13040067

Academic Editor: Hang Gao

Received: 23 February 2022
Accepted: 11 April 2022
Published: 13 April 2022

1. Introduction

In recent years, renewable energy vehicles, EVs and PHEVs are starting to play a significant role in addressing energy shortages and emissions issues as representatives of clean energy vehicles [1,2]. The EVs and PHEVs are also regarded as energy storage units, with the ability to return stored energy to the grid when required [3]. The two-way communication between the electric vehicle and the grid is referred to as vehicle-to-grid (V2G) technology [4]. EVs and PHEVs can have various benefits in this application, such as regulating peak power and shifting peak load. The increased use of battery-powered electric vehicles has increased the need for power generation. Any renewable energy generation system, such as a fuel cell, PV, or wind power generation system can be integrated with an EV to help minimize the burden on the electricity grid. Power converters are in high demand in renewable energy systems, such as V and fuel cells, as well as EV and stand-alone battery-powered installations [5]. The ability to provide high gain to raise the low voltage available from the sources to a usable level is the key requirement of these converters [6]. The DC–DC converter is the most important part of the conventional BC providing good gain, simple structure and continuous input current. Using the traditional

boost topology, it is unable to achieve high gain [7]. Electrical isolation requirements are not met by the BC method. The wide magnitude difference between the input and output puts a lot of strain on the switch, and this topology has a lot of current and voltage ripples, as well as the immense volume and weight of the components [8,9]. These issues can be solved with the help of the MPIBC model.

The MPIBC method is used to improve power converter performance in terms of efficiency, size, conducted electromagnetic emission and transient response [10]. The benefits of interleaving include high power capability, modularity, and improved reliability [11,12]. The interleaved technique is presented to improve the performance of the converter [13]. Based on the interleaving techniques as multi-phase, the switching losses are reduced, in turn, improving the efficiency of the converter [14–16]. The interleaving techniques of multilevel BC are discussed in [17]. Slah F et al. proposed a converter with reduced voltage stress of the components [18]. Kim J H et al. presented a new converter topology to reduce the switching power loss [19]. The input current is distributed equally in the BC inductor, to reduce the transient current and minimize switching during the transient period [20,21]. For high power applications, IBC is used to develop high voltage gain and reduce the power loss and design a new model [22,23]. A hardware setup for two stage IBC is presented. The performance of the converter is compared for two switching frequencies [24]. Lipu M S H et al. presented a comprehensive review of the various converter configurations. The various control schemes for EV applications incorporating optimization techniques are discussed. This paper presents detailed suggestions and challenges for various DC-DC converter topologies [25].

To demonstrate the effectiveness of the presented MPIBC, a comparison with other existing converters is presented in Table 1. The parameters, such as ripple voltage, current, switching frequency, the complexity of the control circuit, high power conversion, and cost are compared for the converters, such as IBC [1], quasi-Z source converter (QZBC) [26], multi-port isolated converter (MPIC) [27]. It is observed that in the presented MPIBC the ripple content, switching frequency and cost is low compared to other converters. The objectives of various converters with their specific outcomes and their benefits are compared in Table 2. It is evident from Table 2 that the presented MPIBC is best compared to other existing converters in terms of low ripple, reduced transients and improved efficiency.

Table 1. MPIBC comparison with other converters.

DC-DC Converter	Ripple (Voltage/Current)	Switching Frequency	Complicity of Control Circuit	High Power Conversion	Cost
IBC [1]	Reasonable	High	Reasonable	Suitable	Low
QZBC [26]	Simple	High	Multifaceted	Suitable	Medium
MPIC [27]	Multifaceted	Low	Multifaceted	Suitable	High
MPIBC	Simple	Low	Reasonable	Suitable	Medium

Table 2. Comparison of objective, outcome and benefits of different converters with MPIBC.

DC-DC Converter	Objective	Outcomes	Benefits
IBC [1]	• Number of passive components are reduced	• Obtains a quick dynamic response • Loses are reduced	• Low ripple current at low output voltage • High switching loss
QZBC [26]	• To achieve a wide range of voltage gain as well as an absolute common ground	• Achieved maximum efficiency	• Switching stress is lower • Component ratings are small

Table 2. *Cont.*

DC-DC Converter	Objective	Outcomes	Benefits
MPIC [27]	• To optimize the system behavior by controlling duty cycle • To reduce overall system losses • To look into dynamic analysis.	• Obtains a quick dynamic response • Power flow can be controlled independently • To obtain high efficiency	• Voltage gain is high. • Low output voltage ripple
MPIBC	• To decrease ripples in output current and inductor current • In order to achieve optimal control and a quick transient response • To reduce overall system losses • To improve the system efficiency	• Obtains a quick dynamic response • In comparison to IBC, the current and voltage ripple are reduced • Low switching stress are obtained • More stable	• Low ripple current at low output voltage • Efficiency improved to compare with IBC • Transients are reduced

The Contribution of this paper is listed as follows:

- The output power and output voltage of the presented converter are 33.38 kW and 500 V. The inductor ripple current is reduced by 25.76%, hence the size and cost of the inductor are also less compared to the existing converter, such as BC and IBC.
- Circuit size reduces due to the reduction in the size of the passive components, which is a major advantage for the EV model.
- Based on the interleaved techniques the total power loss is reduced and the total inductor current is reduced by 26.92% compared to the existing converter.
- The efficiency of the six phase MPIBC is 98.68% compared to the existing converter presented in [28]. The efficiency of the six phase converter presented in [28] is 96.9%. Therefore, the presented converter has improved the efficiency by 1.78%.

2. Multi-Phase Interleaved Boost Converter

2.1. N Phase IBC Schematic Diagram

The MPIBC has an 'N' number of parallel converters are connected and operated by $2\pi/N$ or $360^\circ/N$ radian phase-shifted among the power switches and same duty ratio (D). The MPIBC diagram is shown in Figure 1. In MPIBC, the total power is divided by the number of paralleled converters, and the input and output currents ripples are reduced by 1/N. The inductor currents (I_L) are interleaved using phase shifting between the signals of switches, and the converter's input current (I_{in}) is the sum of inductor currents of N phases. MPIBC has the 'N' inductor (L_1, L_2 … L_N), 'N' diodes (D_1, D_2 … D_N) and 'N' MOSFET switches (S_1, S_2 … S_N). To achieve interleaving, the circuit uses identical inductors, diodes, and capacitors.

2.2. Design Parameter Calcultaion

The values for inductor, capacitor and duty ratio are calculated for MPIBC by using the following Equations (1)–(3):

$$L_N = \left(\frac{D * V_{in}}{f_s * N * \Delta I_{in}}\right), \quad (1)$$

$$C_N = \left(\frac{D * I_{out}}{f_s * N * \Delta V_{out}}\right), \quad (2)$$

$$D = 1 - \left(\frac{V_{in}}{V_{out}}\right), \quad (3)$$

In this paper, 50% duty ratio is used to design of two, three, four and six phases IBC. The parameters of interleaved boost converters are listed in Table 3.

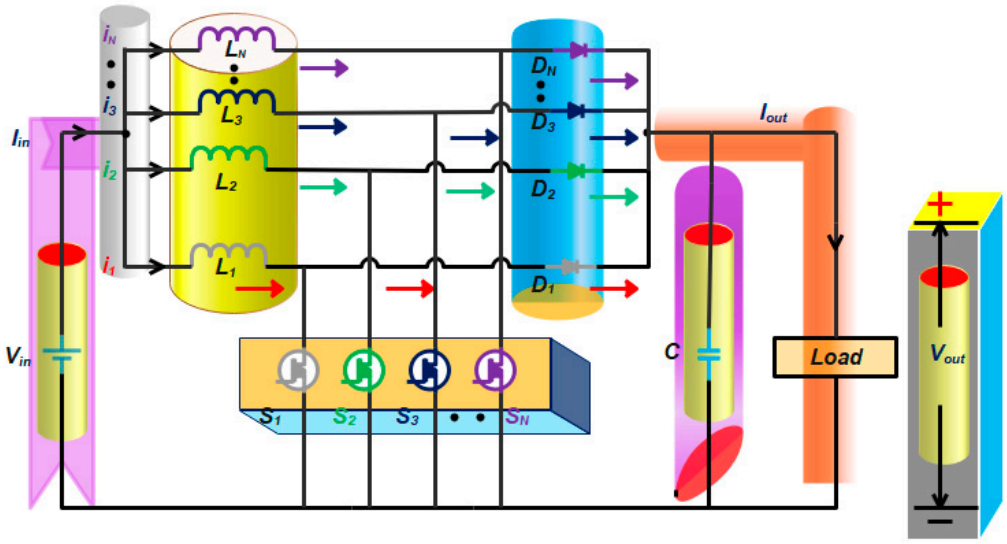

Figure 1. N phase IBC schematic diagram.

Table 3. Parameter values of MPIBC.

Parameter	Value	Unit
Solar PV voltage	20	V
Output voltage	40	V
Output current	1.25	A
Output power	50	W
$L_1 = L_2 = L$ (2 phase IBC)	3.225 m	H
$L_1 = L_2 = L_3 = L$ (3 phase IBC)	2.15 m	H
$L_1 = L_2 = L_3 = L_4 = L$ (4 phase IBC)	1.613 m	H
$L_1 = L_2 = L_3 = L_4 = L_5 = L_6 = L$ (6 phase IBC)	1.075 m	H
C (2 phase IBC)	504 µ	F
C (3 phase IBC)	336 µ	F
C (4 phase IBC)	252 µ	F
C (6 phase IBC)	168 µ	F
R_{load}	32	Ω
L_{load}	120 m	H
Switching frequency (f_s)	31 k	Hz
Input Current Ripple (ΔI_{in})	5%	-
Output Voltage Ripple (ΔV_{out})	2%	-
Duty ratio (D)	50%	-
Drain Source Resistance ($R_{DS(on)}$)	0.045	Ω
Series resistance of Diode (r_D)	0.30	Ω
Internal Series resistance of the inductor (r_L)	0.25	Ω
Internal Series resistance of the capacitor (r_C)	0.05	Ω

The power losses due to MOSFET, diode, inductor and capacitor are calculated using the equations presented in Table 4. Further, Table 4 shows the equation used for input power and efficiency calculation.

Table 4. Loss estimation equation for MPIBC.

Equation	Equation Meaning	Equation Number
$P_{switch} = N * R_{DS(on)} * D * \left[\frac{I_{out}}{N*(1-D)}\right]^2$	*Switching loss*	(4)
$P_{diode} = ((r_D * I_{out}^2) + (V_F * I_{out}))$	*Diode loss*	(5)
$P_{inductor} = r_L * \left[\frac{I_{out}}{(1-D)}\right]^2$	*Inductor loass*	(6)
$P_{capacitor} = r_C * I_{out}^2$	*Capactior loss*	(7)
$P_{input} = P_{output} + P_{switch} + P_{diode} + P_{inductor} + P_{capacitor}$	*Input power*	(8)
$\%\eta = \left(\frac{P_{output}}{P_{input}}\right) \times 100$	*Efficiency*	(9)

3. MPIBC Simulation Result and Discussion

The simulation of two, three, four and six phase IBC is presented in this section for two different input voltages, such as 20 V and 200 V. The power loss calculation and efficiencies are compared for different phases. For an input voltage of 20 V, the output voltage of all phases of MPIBC is shown in Figure 2. From the waveform, the output voltage of two phase IBC is settled at 38.74 V in 0.2 s. The output current and power comparison are depicted as shown in Figures 3 and 4 for an input voltage of 20 V. The output current and power values are 1.211 A and 46.914 W. Similarly, the three, four and six phase IBC output voltages are settled at 38.89 V, 38.96 V, 39.04 V in 0.15 s, 0.11 s and 0.05 s, respectively. The output current and power values of the three, four and six phase are 1.215 A, 1.218 A, 1.22 A and 47.251 W, 47.453 W, 47.628 W, respectively. All inductor currents are depicted as shown in Figure 5.

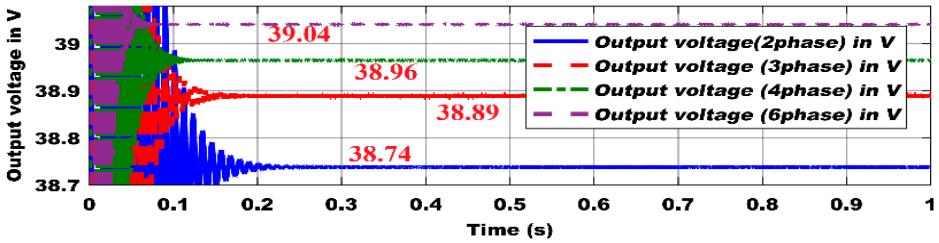

Figure 2. Output voltage comparison of MPIBC at duty cycle of 50%.

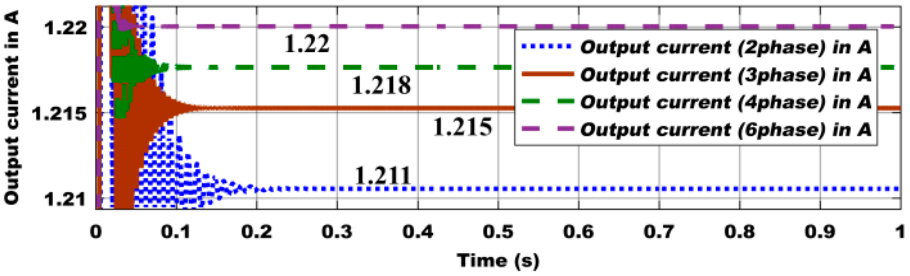

Figure 3. Output current comparison of MPIBC at duty cycle of 50%.

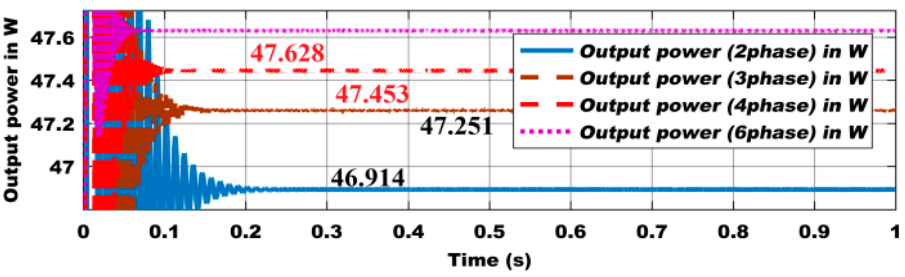

Figure 4. Output power comparison of MPIBC at duty cycle of 50%.

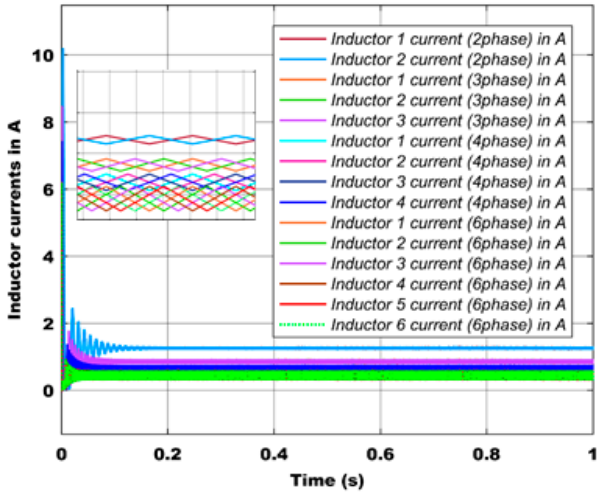

Figure 5. All phases inductor current comparison of MPIBC at duty cycle of 50%.

Based on the MPIBC MATLAB simulation at different phases, the output parameters are listed in Tables 5 and 6. The results presented in Tables 5 and 6 show that if the number of MPIBC phases is increased, the output parameter, such as the voltage, current and power also increases. The reason behind this is the reduction of induction current thereby reducing the switching stress. It indicates that the power losses are decreased while the efficiency of MPIBC is increased.

Table 5. Output parameter values of MPIBC (input voltage: 20 V).

Number of Phases of MPIBC	Output Voltage (V_{out}) in V	Output Current (I_{out}) in A	Output Power (P_o) in W
2	38.74	1.211	46.914
3	38.89	1.215	47.251
4	38.96	1.218	47.453
6	39.04	1.220	47.628

Table 6. Output parameter values of MPIBC (input voltage: 200 V).

Number of Phases of MPIBC	Output Voltage (V_{out}) in V	Output Current (I_{out}) in A	Output Power (P_o) in kW
2	434	13.56	5.887
3	435.7	13.62	5.933
4	436.6	13.64	5.956
6	437.4	13.67	5.979

Power Loss and Efficiency Calculation of MPIBC

The total losses and efficiency are calculated from Equations (4)–(9) for two different input voltages. The values are listed in Tables 7 and 8. The MPIBC total power loss and percentage of efficiency comparison (two phase IBC) are shown in Figures 6 and 7. It clearly shows that, as with the increase in phase, the power loss is reduced and percent efficiency improved. By comparing the four phases of MPIBC, power loss is reduced at the six phase IBC and the efficiencies of 93.82% (at an input voltage is 20 V) and 95.74% (at the input voltage is 200 V) are achieved. It is evident that the inductor and capacitor value (calculated using Equations (1) and (2)) decreases with an increase in the number of phases. The inductor and capacitor value is minimal for the six phase IBC compared to the four phase, three phase and two phase IBC. The inductor and capacitor values for the six phase IBC are 1.075 mH and 168 µF, respectively (refer to Table 1). This reduces the size of the inductor and capacitor significantly.

Table 7. Total power loss and efficiency values of MPIBC (input voltage: 20 V).

Number of Phases of MPIBC	P_{loss} (W)	P_{input} (W)	P_{output} (W)	%Efficiency
2	3.1772	50.1772	46.914	93.66
3	3.1565	50.1565	47.251	93.74
4	3.1448	50.1448	47.453	93.78
6	3.1330	50.1330	47.628	93.82

Table 8. Total power loss and efficiency values of MPIBC (input voltage: 200 V).

Number of Phases of MPIBC	P_{loss} (W)	P_{input} (kW)	P_{output} (kW)	%Efficiency
2	267.347	6.154	5.887	95.66
3	266.880	6.199	5.933	95.71
4	266.263	6.222	5.956	95.72
6	266.010	6.245	5.979	95.74

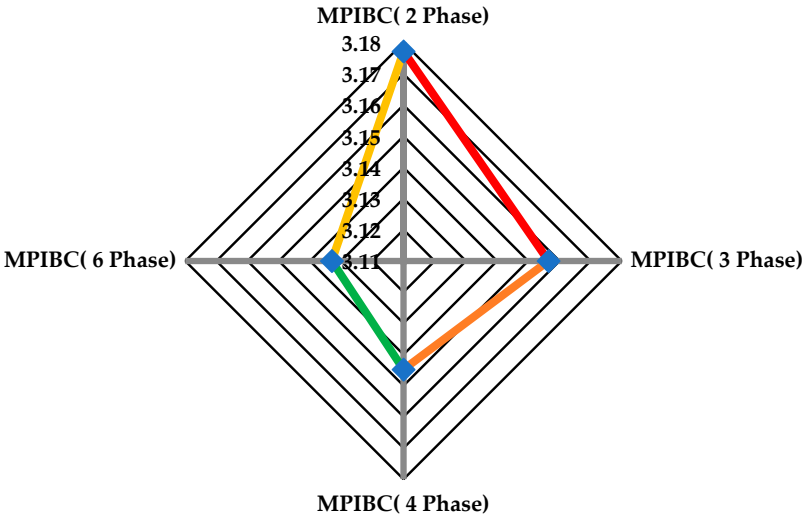

Figure 6. Total power loss comparison of MPIBC (input voltage: 20 V).

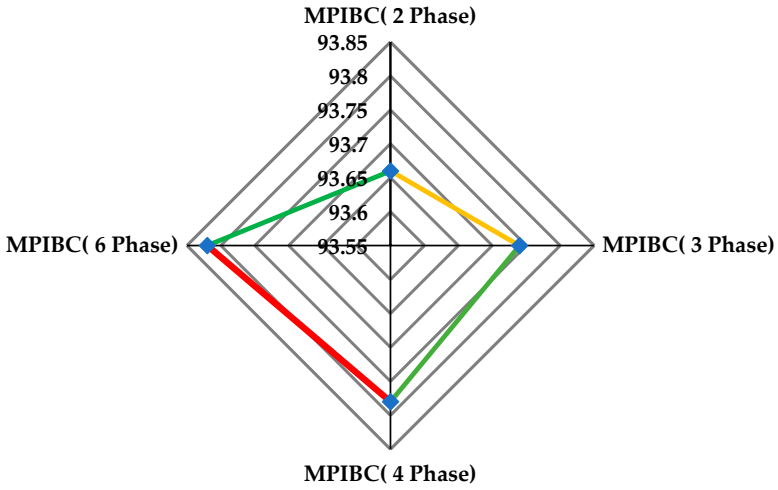

Figure 7. %Efficiency comparison of MPIBC (input voltage: 20 V).

To validate the results obtained from the MPIBC, a comparison is made with the existing converters, such as BC and IBC. The passive components, such as the inductor and capacitor are designed for all the converters taken for comparison. The common parameters used for BC and IBC are compared with the six phase MPIBC converter. From Table 9, it is clear that the MPIBC provides better output voltage and output power. The output voltage and output powers are 500 V and 34.38 kW, respectively. Inductor current reduces by 26.92%. The MPIBC reduces inductor and capacitor values significantly. The inductor and capacitor values of the six phase MPIBC are 66.67 µH and 168 µF, respectively. Therefore, it is concluded that the six phase MPIBC is better than the existing converter.

Table 9. MPIBC comparison with existing converter.

Parameters	BC [1]	IBC [1]	MPIBC
Input Voltage (V)	200	200	200
Output Voltage (V)	400	400	500
Number of Phase	1	4	6
Output Power (kW)	30	30	34.38
Switching Freqency (kHz)	20	20	20
Inductor Current (A)	250	250	182.7
Inductor (µH)	400	100	66.67
Capactior (µF)	780	195	168
Duty Cycle	0.5	0.5	0.5
Inductor Current Ripple (A)	12.5	12.5	9.28

To validate specifically the six phase MPIBC, the presented converter is compared with the existing converter presented in [28]. The comparison result shows that the presented converter has an efficiency of 98.6% which is better than the existing converter. This comparison is presented in detail with other parameters in Table 10.

Table 10. Six phase MPIBC comparison with existing converter.

Parameters	Six Phase IBC [28]	Six Phase MPIBC
Input Voltage (V)	24	24
Number of Phase	6	6
Switching Freqency (kHz)	25	25
Duty Cycle	0.6	0.6
Output Voltage (V)	207	213.8
Output Power (W)	453	487.6
%Efficiency	96.90	98.68

4. Hardware Setup for MPIBC

Figure 8 shows a block diagram of a two phase IBC based EV. Two phase IBC hardware is developed by the two identical inductors, two diodes and two MOSFET switches. The filter circuit is reduced to harmonic contents. This EV hardware prototype was performed on a 5 V input supply. To invert a signal, transistors are used, because IBC needs a 180° phase shift for the two phase interleaved technique.

4.1. Two Phase IBC Hardware Results and Discussion

A hardware prototype was developed and assembled to validate the actual performance of the two phase IBC. The two phase IBC hardware is designed for 5 kHz and 10 kHz switching frequencies. The EV hardware prototype for MPIBC (two phase) is shown in Figure 9. The supply voltage range is considered to be 0–5 V. The converter is fed with a nominal voltage of 5 V. Figure 10 depicts the two phase IBC output voltage.

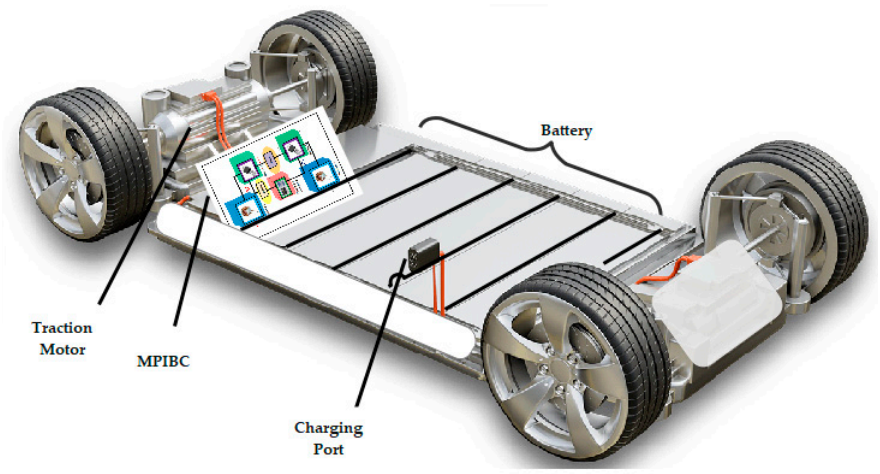

Figure 8. MPIBC (Two phase) hardware circuit diagram.

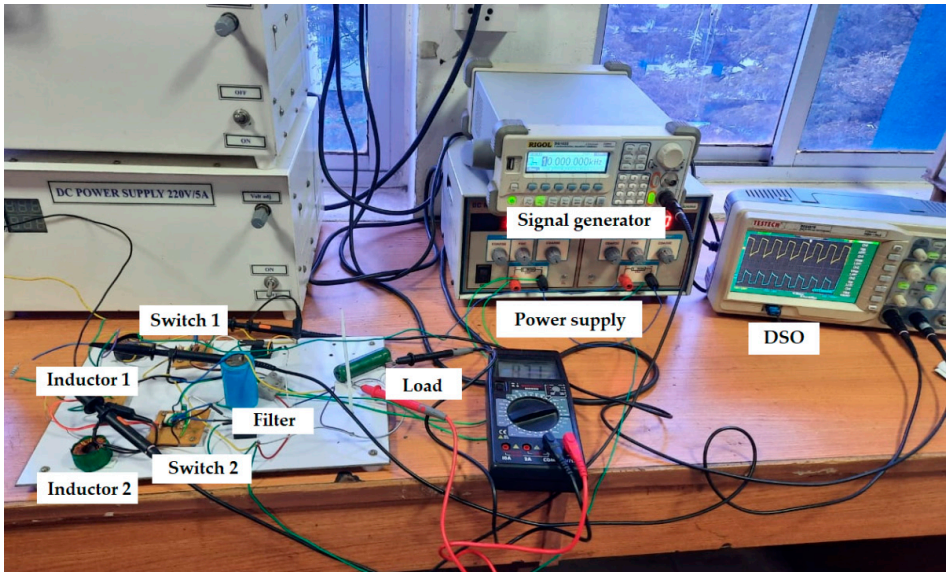

Figure 9. Hardware prototype for MPIBC (two phase).

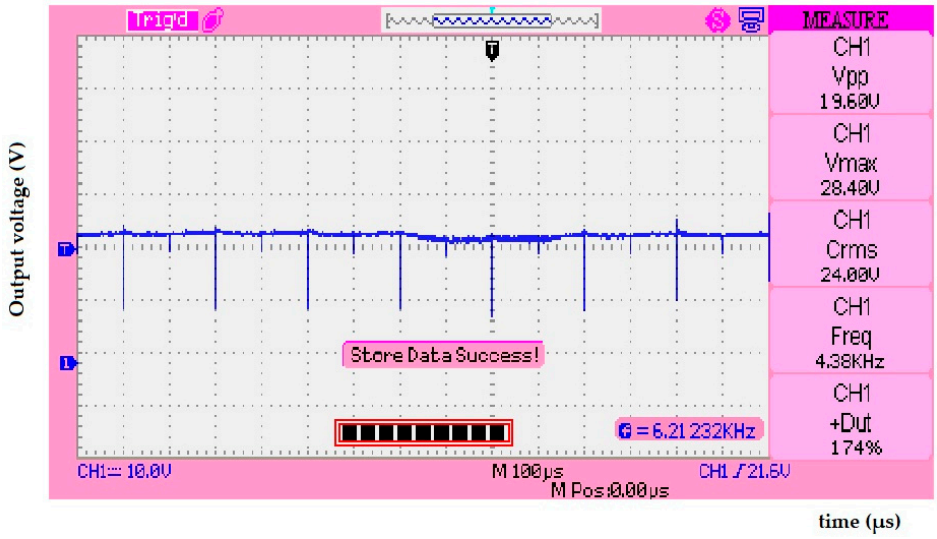

Figure 10. Load output voltage waveform.

The output voltage comparison at different duty ratios of both switching frequencies 5 kHz and 10 kHz are listed in Table 11. Figures 11 and 12 indicate that the duty ratio increases simultaneously as the load voltage increases.

Table 11. Comparison of output voltages at different duty cycles and with f_s = 5 kHz and f_s = 10 kHz.

V_{in} (V)	Switching Frequency f_s = 5 kHz				Switching Frequency f_s = 10 kHz			
	V_{out} (V) at D = 0.3	V_{out} (V) at D = 0.4	V_{out} (V) at D = 0.5	V_{out} (V) at D = 0.7	V_{out} (V) at D = 0.3	V_{out} (V) at D = 0.4	V_{out} (V) at D = 0.5	V_{out} (V) at D = 0.7
0.5	1.2	1.4	1.2	1.2	1.4	1.2	1	1.6
1	2.6	2.8	2.8	3.2	2.8	3.2	2	3.2
1.5	4.4	4.2	4.4	4.4	4.4	4	4.2	5
2	6	5.4	5.6	6	5.6	5.8	6.4	6.4
2.5	6.8	7.2	7.2	7.6	7.2	7.4	8.2	8.2
3	8	8.6	8.8	9.4	8.2	9.6	9.2	10.8
3.5	9.8	9.8	10.2	11	9.4	10	11.6	11.8

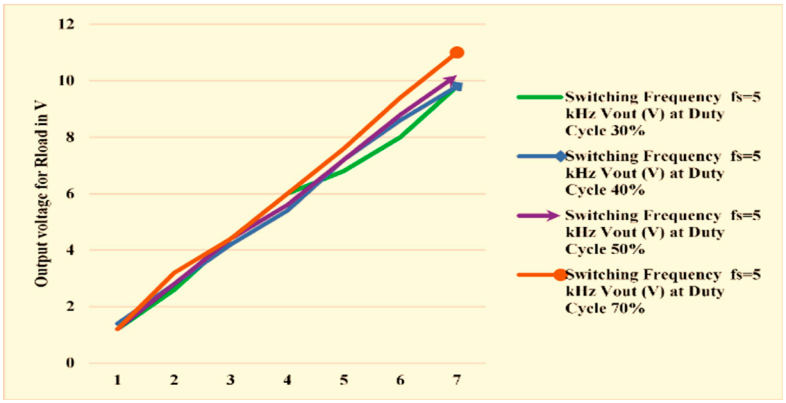

Figure 11. Output voltage comparison at different duty cycles and f_s = 5 kHz.

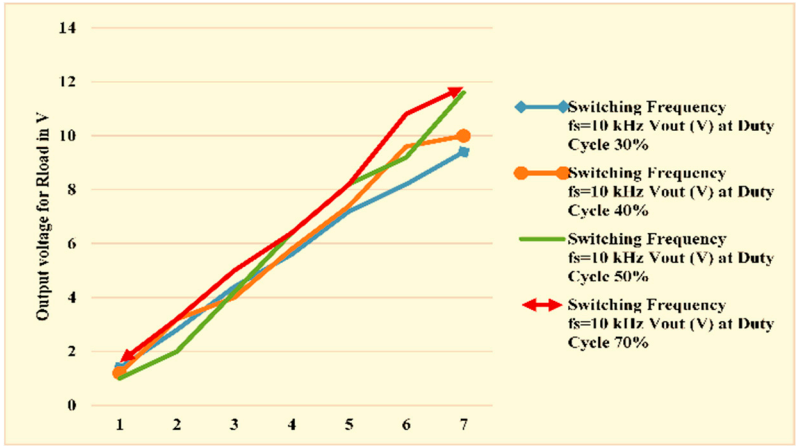

Figure 12. Output voltage comparison at different duty cycles and f_s = 10 kHz.

Table 12 compares the experimental results of the IBC-based EV that was implemented in terms of output current, output voltage, and output power at two switching frequencies of 5 kHz and 10 kHz also maintained at a duty cycle of 50%.

Table 12. Output voltage, current and power comparison at f_s = 5 kHz and f_s = 10 kHz.

V_{in} (V)	Switching Frequency f_s = 5 kHz			Switching Frequency f_s = 10 kHz		
	V_{out} (V)	I_{out} (mA)	P_{out} (mW)	V_{out} (V)	I_{out} (mA)	P_{out} (mW)
0.5	1.4	14	19.6	1.4	14	19.6
1.1	2.3	23	52.9	2.8	28	78.4
1.5	4.3	43	184.9	3.6	36	129.6
2	5.12	51.2	262.14	4.4	44	193.6
2.5	7.38	73.8	544.64	6.2	62	384.4
3	9.46	94.6	894.92	7.4	74	547.6
3.5	9.83	98.3	966.29	8.6	86	739.6
4	11.22	112.2	1258.88	10.2	102	1040.4
4.5	12.54	125.4	1572.52	11	110	1210
5	13.2	132	1742.4	12.4	124	1537.6

Based on the output current, voltage and power comparison at two different switching frequencies, the load voltage is boosted more at 5 kHz switching frequencies, and the value of the output voltage is 13.2 V. This output voltage is 1.06 times more than the output voltage at 10 kHz switching frequency it is shown in Figure 13. If the supply voltage increases the output current also increased. To achieve more output power at the switching frequency of 5 kHz compared with a switching frequency of 10 kHz.

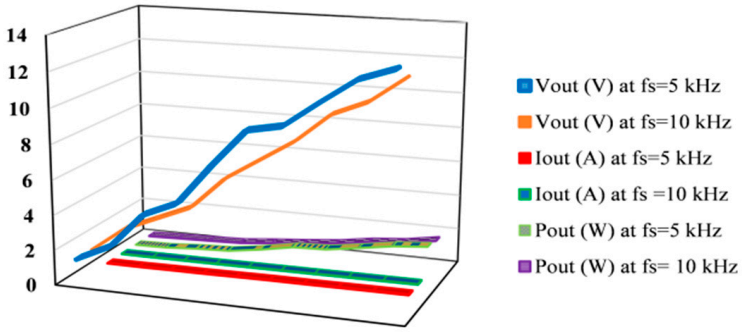

Figure 13. Output voltage, current and power comparison at switching frequencies f_s = 5 kHz and f_s = 10 kHz.

Inductor voltage, current, and power losses at two different switching frequencies with a 50% duty cycle are listed in Tables 13 and 14. At 5 kHz switching frequency the two phase IBC's two inductor voltage, current and power comparison are shown in Figure 14. The comparison of inductor currents indicates that the second inductor current is minimal. At a 10 kHz switching frequency and duty cycle of 50%, the two phase IBC's two inductor voltage, current and power comparison are shown in Figure 15. Over the two phase IBC power loss is minimum at f_s = 5 kHz compared with f_s = 10 kHz.

Table 13. Inductor voltage, current and power loss at f_s = 5 kHz and D = 50%.

$Inductor_1$ Voltage (V)	$Inductor_2$ Voltage (V)	I_{L1} (A)	I_{L2} (A)	P_{L1} (W)	P_{L2} (W)
0.28	0.28	0.35	0.23	0.098	0.065
0.36	0.36	0.45	0.30	0.162	0.108
0.72	0.56	0.9	0.47	0.648	0.261
0.76	0.68	0.95	0.57	0.722	0.385
0.96	0.84	1.2	0.70	1.152	0.588

Table 13. *Cont.*

$Inductor_1$ Voltage (V)	$Inductor_2$ Voltage (V)	I_{L1} (A)	I_{L2} (A)	P_{L1} (W)	P_{L2} (W)
1.16	1.04	1.45	0.87	1.682	0.901
1.32	1.2	1.65	1.00	2.178	1.200
1.44	1.28	1.8	1.07	2.592	1.365
1.56	1.48	1.95	1.23	3.042	1.825
1.64	1.64	2.05	1.37	3.362	2.241

Table 14. Inductor voltage, current and power loss at f_s = 10 kHz and D = 50%.

$Inductor_1$ voltage (V)	$Inductor_2$ voltage (V)	I_{L1} (A)	I_{L2} (A)	P_{L1} (W)	P_{L2} (W)
0.360	0.240	0.450	0.200	0.162	0.048
0.440	0.280	0.550	0.233	0.242	0.065
0.560	0.400	0.700	0.333	0.392	0.133
0.720	0.520	0.900	0.433	0.648	0.225
0.920	0.720	1.150	0.600	1.058	0.432
1.000	0.760	1.250	0.633	1.250	0.481
1.200	0.960	1.500	0.800	1.800	0.768
1.320	1.040	1.650	0.867	2.178	0.901
1.520	1.160	1.900	0.967	2.888	1.121
1.560	1.280	1.950	1.067	3.042	1.365

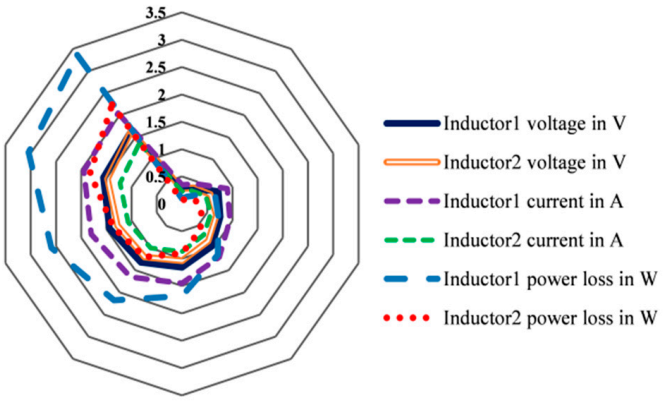

Figure 14. Inductor voltage, current and power loss comparison at f_s = 5 kHz and D = 50%.

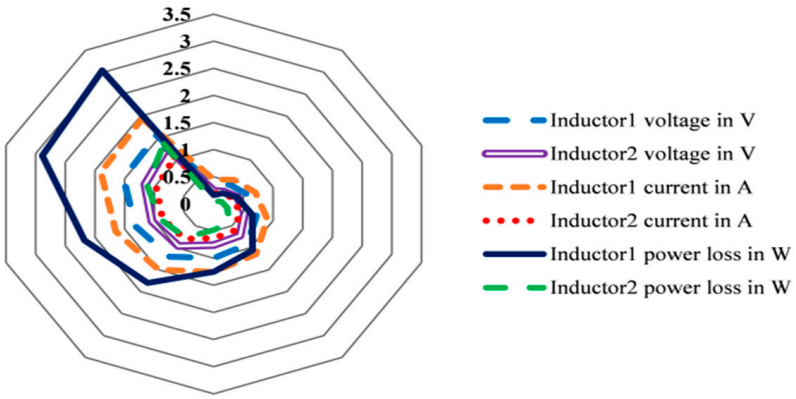

Figure 15. Inductor voltage, current and power loss comparison at f_s = 10 kHz and D = 50%.

4.2. Six Phase IBC Hardware Results and Discussion

A hardware prototype was developed and assembled to validate the actual performance of the six phase IBC. The six phase IBC hardware is designed for a 5 kHz switching frequency. The EV hardware prototype for MPIBC (six phase) is shown in Figure 16. The supply voltage range is considered to be 0–5 V. The converter is fed with a nominal voltage of 5 V. Figure 17 depict the six phase MPIBC pulses waveform and Figure 18 shows the six phase MPIBC output voltage waveform.

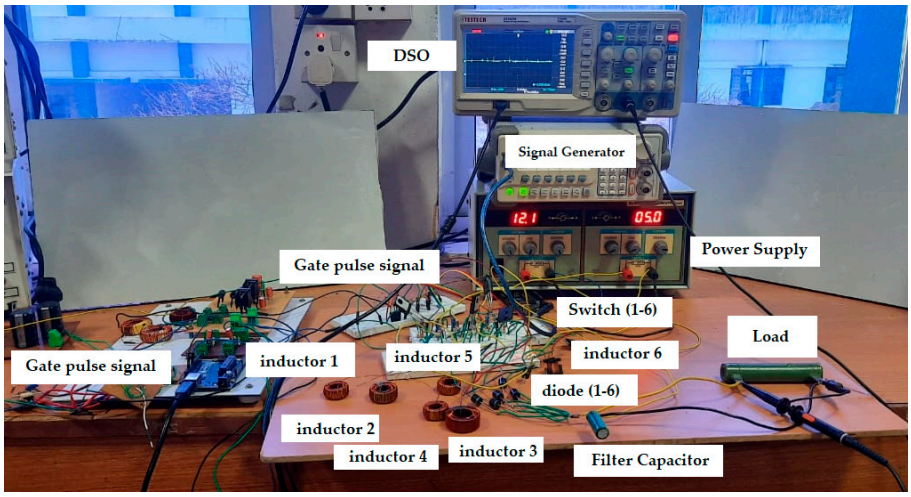

Figure 16. Hardware prototype MPIBC (six phase).

Figure 17. Pulse waveform MPIBC (six phase).

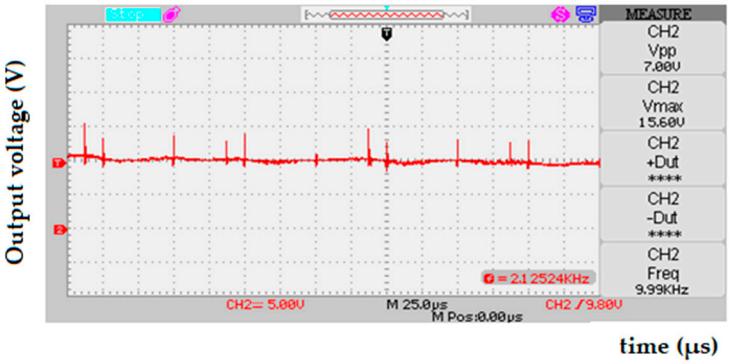

Figure 18. Output voltage waveform MPIBC (six phase). **** Duty Cycle = 0.5.

The output current, output voltage, and output power of MPIBC (six phase) at a switching frequency of 5 kHz are listed in Table 15; if also maintained at a duty cycle of 50%.

Table 15. Output voltage, current and power at f_s = 5 kHz.

V_{in} (V)	Switching Frequency f_s = 5 kHz		
	V_{out} (V)	I_{out} (mA)	P_{out} (W)
0.5	11	110	1.21
1.0	11.6	116	1.34
1.5	11.8	118	1.39
2	12.1	121	1.46
2.5	12.4	124	1.53
3	12.8	128	1.64
3.5	13.1	131	1.72
4	13.6	136	1.85
4.5	14	140	1.96
5	15.6	156	2.43

Based on the output current, voltage and power comparison at 5 kHz switching frequency of six phase IBC, the values of output voltage is boosted 15.6 V at input voltage of 5 V. The output voltage and output power values are more for the six phase hardware setup compare with two phase IBC hardware results. The six phase IBC output voltage and output power values are 1.181 times and 1.409 times higher than the two phase IBC hardware setup (refer Tables 11 and 14).

5. Conclusions

A simulation model and hardware implementation of the MPIBC-based EV is discussed in this paper. MPIBC based EV simulation is carried out for four different phases of IBC and two, three, four and six phases of MPIBC. The simulation is performed with an input voltage of 20 V and the boosted output voltage is 39.04 V. By comparing four different phases of MPIBC, the output voltage, current and power values quickly settle for the six phase model of MPIBC. The power loss calculation of four models reveals that the six phase IBC has minimum loss with an efficiency of 93.82% for 20 V input voltage. Further, efficiency of 95.74% is obtained for 200 V input voltage. The effectiveness of the six phase MPIBC is validated by comparing it with the existing converters, such as BC and IBC. Further, six phase MPIBC is specifically compared with the existing converter. The presented converter provides efficiency of 98.68% which is 1.78% better than the existing converter. The two phases of the MPIBC hardware prototype are fabricated and various comparative analyses are performed in the hardware prototype. The output power is increased at a 5 kHz switching frequency compared to 10 kHz as per the qualitative study. The performance and features of the two phases of the MPIBC system under various duty cycle conditions have been analyzed. The simulation and experimental results show that the MPIBC can reduce the switching stresses and increases efficiency. By using the proposed two phase and six phase fabricated MPIBC hardware, the EV output can be easily controlled. The presented converter provides better performance, smooth speed control and improved battery life. The proposed converter can be used in various other applications, such as battery charging, fuel cells, solar panels, PHEV, etc.

Author Contributions: Conceptualization, S.S. and Z.R.; methodology, S.S.; software, S.S.; validation, Z.R. and S.C.; formal analysis, E.S.; investigation, resources, S.S. and S.P.; data curation, U.S.; writing—original draft preparation, S.S.; writing—review and editing, Z.R., S.C., S.P. and U.S.; visualization, S.S.; supervision, Z.R. and S.P.; project administration, Z.R. and S.C.; funding acquisition, U.S. All authors have read and agreed to the published version of the manuscript.

Funding: This research received no external funding.

Institutional Review Board Statement: Not applicable.

Informed Consent Statement: Not applicable.

Data Availability Statement: Not applicable.

Acknowledgments: The authors would like to thank the support of Renewable Energy Lab, Prince Sultan University for technical guidance and contributions to this work.

Conflicts of Interest: The authors declare no conflict of interest.

Nomenclature

N	no phase for MPIBC
D	duty ratio
V_{in}	input voltage (V)
f_s	switching frequency (Hz)
ΔI_{in}	input current ripple
ΔV_{out}	output voltage ripple
I_{out}	output current (A)
V_{out}	output voltage (V)
L_N	inductance at Nth phase (H)
C_N	capacitance at Nth phase (H)
$R_{DS(on)}$	drain source resistance (Ω)
r_D	series resistance of diode (Ω)
V_F	diode forward voltage (V)
r_L	internal series resistance of the inductor (Ω)
r_C	internal Series resistance of the capacitor (Ω)
P_{input}	input power (W)
P_{output}	output power (W)
P_{switch}	losses due to switching operation (W)
P_{diode}	losses due to diode (W)
$P_{inductor}$	losses due to diode (W)
$P_{inductor}$	capacitor power loss (W)
η	efficiency

References

1. Chakraborty, S.; Vu, H.N.; Hasan, M.M.; Tran, D.D.; Baghdadi, M.E.; Hegazy, O. DC-DC converter topologies for electric vehicles, plug-in hybrid electric vehicles and fast charging stations: State of the art and future trends. *Energies* **2019**, *12*, 1569. [CrossRef]
2. Elsied, M.; Salem, A.; Oukaour, A.; Gualous, H.; Chaoui, H.; Youssef, F.T.; Belie, D.; Melkebeek, J.; Mohammed, O. Efficient power-electronic converters for electric vehicle applications. In Proceedings of the 2015 IEEE Vehicle Power and Propulsion Conference (VPPC), Montreal, QC, Canada, 19–22 October 2015; pp. 1–6.
3. Lai, C.M. Development of a novel bidirectional DC/DC converter topology with high voltage conversion ratio for electric vehicles and DC-microgrids. *Energies* **2016**, *9*, 410. [CrossRef]
4. Zahira, R.; Amirtharaj, S.; Selvarani, M.; Lakshmi, D. Design of MOSFET Inverter for a Grid Connected Photovoltaic System. In Proceedings of the AICTE Sponsored National Conference on Recent Advances in On-Board Ship Automation (RAOBSA-2019), Chennai, India, 26–27 September 2019; pp. 253–256.
5. Guo, J.; Rodriguez, R.; Gareau, J.; Schumacher, D.; Alizadeh, M.; Azer, P.; Bauman, J.; Bilgin, B.; Emadi, A. A Comprehensive Analysis for High-Power Density, High-Efficiency 60 kW Interleaved Boost Converter Design for Electrified Powertrains. *IEEE Trans. Veh. Technol.* **2020**, *69*, 7131–7145. [CrossRef]
6. Sunddararaj, S.P.; Rangarajan, S.S.; Subashini, N.; Subramaniam, U.; Collins, E.R.; Senjyu, T. A novel T-Type Multilevel Inverter for Electric Vehicle and Grid-connected applications. In Proceedings of the 2021 7th International Conference on Electrical Energy Systems (ICEES), Chennai, India, 11–13 February 2021; pp. 166–170.
7. Subramaniam, U.; Ganesan, S.; Bhaskar, M.S.; Padmanaban, S.; Blaabjerg, F.; Almakhles, D.J. Investigations of AC Microgrid Energy Management Systems Using Distributed Energy Resources and Plug-in Electric Vehicles. *Energies* **2019**, *12*, 2834. [CrossRef]
8. Sunddararaj, S.P.; Rangarajan, S.S.; Subramaniam, U.; Collins, E.R.; Senjyu, T. A new topology of DC-DC Converter with Bidirectional Power Flow Capability Coupled with a Nine Multilevel Inverter for EV Applications. In Proceedings of the 2021 7th International Conference on Electrical Energy Systems (ICEES), Chennai, India, 11–13 February 2021; pp. 177–182.
9. Dawidziuk, J. Review and comparison of high efficiency high power boost DC/DC converters for photovoltaic applications. *Bull. Pol. Acad. Sci. Tech. Sci.* **2011**, *59*, 499–506. [CrossRef]
10. Wang, L.; Jiao, H.; Yang, G.; Li, J.; Zhang, Y. Current sharing compensation control method for interleaved current source isolated bidirectional DC/DC converters. *J. Power Electron.* **2022**, *22*, 1–9. [CrossRef]
11. Zhang, Z.; Xie, S.; Wu, Z.; Xu, J. Soft-switching and low conduction loss current-fed isolated bidirectional DC–DC converter with PWM plus dual phase-shift control. *J. Power Electron.* **2020**, *20*, 664–674. [CrossRef]

12. Geetha, E.; Maddah, M.; Khosravi, M.M.; Kokabi, A.; Samavatian, V. Dynamic enhancement of interleaved step-up/step-down DC-DC converters using passive damping networks. *J. Power Electron.* **2020**, *20*, 657–663. [CrossRef]
13. Lai, C.M.; Pan, C.T.; Cheng, M.C. High-efficiency modular high step-up interleaved boost converter for DC-microgrid applications. *IEEE Trans. Ind. Appl.* **2011**, *48*, 161–171. [CrossRef]
14. Subramaniam, U.; Palanisamy, K.; Deb, S.; Paul, S.; Bharadwaj, S.C.; Dutta, N. A Solution to Fast Battery Charging Technology With Bi-Directional Series Parallel Resonant Converter LCC In Grid to Vehicle Ambient. In Proceedings of the Innovations in Power and Advanced Computing Technologies (i-PACT), Vellore, India, 22–23 March 2019; pp. 1–6.
15. Henn, G.A.; Silva, R.N.A.L.; Praca, P.P.; Barreto, L.H.; Oliveira, D.S. Interleaved-boost converter with high voltage gain. *IEEE Trans. Power Electron.* **2010**, *25*, 2753–2761. [CrossRef]
16. Sunddararaj, S.P.; Rangarajan, S.S.; Subramaniam, U.; Collins, E.R.; Senjyu, T. Performance of P/PI/PID Based controller in DC-DC Converter for PV applications and Smart Grid Technology. In Proceedings of the 2021 7th International Conference on Electrical Energy Systems (ICEES), Chennai, India, 11–13 February 2021; pp. 171–176.
17. Iqbal, A.; Bhaskar, M.S.; Meraj, M.; Padmanaban, S.; Rahman, S. Closed-loop control and boundary for CCM and DCM of nonisolated inverting N× multilevel boost converter for high-voltage step-up applications. *IEEE Trans. Ind. Electron.* **2019**, *67*, 2863–2874. [CrossRef]
18. Abhiram, J.S.; Kumar, S.S.; Jayaprakash, P.; Subramaniam, U. Design and Analysis of a High Step-Up DC-DC Converter Fed Grid Connected Fuel Cell System. In Proceedings of the 2020 International Conference on Power Electronics and Renewable Energy Applications (PEREA), Kannur, India, 27–28 November 2020; pp. 1–6.
19. Kim, J.H.; Jung, Y.C.; Lee, S.W.; Lee, T.W.; Won, C.Y. Power loss analysis of interleaved soft switching boost converter for single-phase PV-PCS. *J. Power Electron.* **2010**, *10*, 335–341. [CrossRef]
20. Wang, S.; Wang, Y.; Wang, F. Low current ripple high step-up interleaved boost converter with switched-capacitors and switched-inductors. *J. Power Electron.* **2021**, *21*, 1646–1658. [CrossRef]
21. Murali, A.; Wahab, R.S.; Gade, C.S.R.; Annamalai, C.; Subramaniam, U. Assessing Finite Control Set Model Predictive Speed Controlled PMSM Performance for Deployment in Electric Vehicles. *World Electr. Veh. J.* **2021**, *12*, 41. [CrossRef]
22. Meraj, M.; Bhaskar, M.S.; Iqbal, A.; Al-Emadi, N.; Rahman, S. Interleaved multilevel boost converter with minimal voltage multiplier components for high-voltage step-up applications. *IEEE Trans. Power Electron.* **2020**, *35*, 12816–12833. [CrossRef]
23. Ghaffarpour, S.H.; Afjei, S.E.; Salemnia, A. A novel soft-switched interleaved high step-up DC–DC converter for high-efficiency conversion. *Int. J. Circuit Theory Appl.* **2021**, *49*, 2515–2532. [CrossRef]
24. Suresh, S.; Zahira, R. Hardware Implementation of Two Stage Interleaved Boost Converter for Electric Vehicle Application. *Int. J. Veh. Struct. Syst.* **2021**, *13*, 373–377. [CrossRef]
25. Lipu, M.S.H.; Faisal, M.; Ansari, S.; Hannan, M.A.; Karim, T.F.; Ayob, A.; Hussain, A.; Miah, M.; Saad, M.H.M. Review of Electric Vehicle Converter Configurations, Control Schemes and Optimizations: Challenges and Suggestions. *Electronics* **2021**, *10*, 477. [CrossRef]
26. Zhang, Y.; Liu, Q.; Li, J.; Sumner, M. A common ground switched Quasi- Z –Source Bidirectional DC-DC Converter with wide voltage –Gain range for EVs with Hybrid Energy Sources. *IEEE Trans. Ind. Electron.* **2017**, *65*, 5188–5200. [CrossRef]
27. Zhao, C.; Round, S.D.; Kolar, J.W. An isolated three- port bidirectional DC-DC converter with decoupled with power flow management. *IEEE Trans. Power Electron.* **2018**, *23*, 2443–2453. [CrossRef]
28. Maalandish, M.; Hosseini, S.H.; Ghasemzadeh, S.; Babaei, E.; Alishah, R.S.; Jalilzadeh, T. Six-phase interleaved boost dc/dc converter with high-voltage gain and reduced voltage stress. *IET Power Electron.* **2017**, *10*, 1904–1914. [CrossRef]